Scientific paper

Corrosion Inhibition Behavior and Adsorption Mechanism of Ethyl Acetate Extract from *Scorzonera Undulata* for Carbon Steel in 1 M HCl Solution

Asma Soudani,^{1,2} Brahim Harkati,² Abdelkader Nadjem³ and Abdelkrim Gouasmia¹

¹ Laboratory of Organic Materials and Heterochemistry, Larbi Tebessi University, 12002, Tebessa – Algeria.

² Laboratory of Bioactive Molecules and Applications, Larbi Tebessi University, 12002, Tebessa – Algeria.

³ Laboratory of Electrical Engineering, Larbi Tebessi University, 12002, Tebessa – Algeria.

* Corresponding author: E-mail: asma.soudani@univ-tebessa.dz

Received: 09-09-2022

Abstract

For carbon steel X70 in a 1 M hydrochloric acid solution, *Scorzonera undulata* acetate extract (SUAc) was investigated as an ecological corrosion inhibitor. The anti-corrosion effect of *Scorzonera undulata* extract is studied using potentio-dynamic polarization analysis and electrochemical impedance spectroscopy (EIS). The polarization curves clearly show that the extract is an excellent mixed inhibitor. Our findings show that the maximum inhibition efficiency of 83% has been found with inhibitor concentration up to 400 mg/L at 298 Kelvin. The Langmuir isotherm is followed by the inhibitor's adsorption on the steel surface and physical adsorption was discovered to be the mechanism. To understand the inhibitory mechanism, thermodynamic parameters (ΔG°_{ads}) and activation parameters (E_a , ΔH_a , and ΔS_a) were determined. Scanning electron microscopy (SEM) and X-ray photoelectron spectrometry studies of the surface chemistry and morphology are included to this investigation. The results obtained from chemical and electrochemical measurements, confirm that a protective film is formed on the carbon steel surface.

Keywords: Scorzonera undulata; corrosion inhibitor; scanning electron microscopy; X-ray photoelectron spectrometry.

1. Introduction

Metal corrosion is a natural phenomenon that affects, causes damage and change the chemicaland physical properties of these metals. Many investigations and scientific research have been conducted on this phenomenon, which is considered as one of the major industrial issues. Metal contact with hydrochloric acid can be harmful and lead to strong corrosion during certain processes such as cleaning, descaling, pickling or even transportation. Due to their p-electron system and heteroatoms such S, P, N, and O, the organic molecules utilized as inhibitors are adsorbed on the metal surface.²⁻⁴ This adsorption is either chemical (chemisorption) or physical (physisorption). After a lot of research and investigation looking into the best and the most effective methods of protecting metals from corrosion, it has been found that the use of inhibitors is one of the most practical methods and one of the best options available.⁵⁻⁶ Although synthetic chemicals have good inhibitory efficiency, their application is restricted due to their higher cost, non-biodegradability, and adverse effects on both humans and environment. Recent studies are increasingly focusing on corrosion inhibition properties and working to create stable, non-toxic organic compounds in an attempt to overcome these drawbacks. The use of affordable, biodegradable, natural products is crucial for protection. Plant extracts are typically produced using straightforward extraction techniques and exhibit good acidic medium inhibitory characteristics. 7 Scorzonera undulata is a genus belonging to the sunflower family (Asteraceae). With the use of LCMS-MS analysis, we started a preliminary study on the acetate extract of Scorzonera undulata, and we noted the presence of three major molecules: 3',4',5-trihydroxy-6, 7-dimethoxy-flavone (Cirsiliol), 4,5-Dihydroxy-6, 7-dimethoxyflavone (Skrofulein), 2S,3S, 4aS,5aS,9aS,10aS)-3,5a,10a- Tris(methoxymethyl)-2-methyldecahydro-2H-dipyrano[3,2-b:2,3'-e] pyran-3-ol). Using potentiodynamic polarization and electrochemical impedance methods, the effect of the ethyl acetate extract of *Scorzonera undulata* on adsorption and corrosion inhibition was investigated in this work. This investigation is complemented morphological and surface chemistry studies using scanning electron microscopy and X-ray photoelectron spectrometry.

2. Experimental

2. 1. Preparation of Solutions

The corrosive solution used in this study is an acidic solution (1 M HCl), obtained by diluting concentrated hydrochloric acid (37%) with distilled water and adding different concentrations of ethyl acetate extract from the *Scorzonera undulata*.

2. 2. Specimen Preparation

X70 steel is the substance utilized to make the working electrode. Table 1 lists the chemical composition and mechanical characteristics.

vonoid aglycones, primarily monoglycosides, for the organic phase. In order to extract the flavonoids di and triglycosides in particular, the residual aqueous phase is combined with n-butanol. The majority of the most polar glycosylated flavonoids are present in the final aqueous phase. Low-pressure evaporation is employed to concentrate the four collected phases.^{8–9}

3. Methods

3. 1. Electrochemical Tests

In a Pyrex cell with a typical three-electrode configuration steel as the working electrode (ET), platinum as the auxiliary electrode and a saturated Hg/Hg₂Cl₂/KCl calomel electrode (ECS) as the reference electrode, the electrochemical experiments are carried out. The latter is equipped with a Luggin capillary, the end of which is placed opposite the working electrode. The measurements are carried out with a set comprising a PGZ301 potentiostat-galvanostat, type Radiometer, associated with the "voltamaster 4" software. Before plotting the curves, the working electrode is held at its drop potential for 60 minutes. Electrochemical impedance spectroscopies (EIS)

Table 1. Chemical composition and mechanical properties of X70 raw rolled steel

Element	С	Si	Mn	P	S	Cr	Ni	Mo	Al	Sn	Cu	Nb	Ti	V	(Nb+Ti+V)
Composition	70	350	1580	0	3	41	32	9	46	1	22	57	4	80	141

2. 3. Extraction

Markham's approach (1982) is followed for the extraction procedure, with a change made in response to Bruneton's method (1993). It is based on how well flavonoids dissolve in organic solvents. The two primary steps in this process are the first extraction phase, which uses methanol to solubilize the flavonoids, and the second extraction phase, which uses diethyl ether to extract free genins, ethyl acetate to extract monoglycosides, and n-butanol to extract free genins (to solubilize di and triglycosides). Flavonoid extraction is carried out from the finely ground dry matter with methanol. The macerate is filtered on a Büchner under reduced pressure and then subjected to low-pressure evaporation at 38°C (Rota Vapor, Büchi 461, Germany). Three successive washings with petroleum ether (v/v) liberate the filtrate of waxes, lipids, and chlorophyll to produce an aqueous phase. The aqueous phase is combined with diethyl ether (v/v) to create an organic phase that contains the flavonoids aglycones and the methoxylated aglycones, which are used to separate the flavonoids into aglycones, monoglycosides, di-, and triglycosides. Three ethyl acetate extractions are then applied to the remaining aqueous phase in order to recover some flawere performed in the frequency range of 10 kHz to 10 mHz with a sinusoidal voltage amplitude of 10 mV at open circuit potential (OCP). The potentiodynamic polarization test was performed in the potential range and at a slew rate of -250 to +250 mV relative to the OCP and at 1 mV/s, respectively. We first plotted the electrochemical impedance spectroscopy and potentiodynamic polarization spectroscopy curves.

3. 2. Scanning Electron Microscopy (SEM)

After being submerged in a corrosive solution (1M HCl) for two hours at 293 K with and without the addition of the ideal concentration of ethyl acetate extract, the surface morphology of carbon steel was examined using SEM analysis (JEOLJSM-6360LV).

3. 3. X-ray Photoelectron Spectrometry

The X-ray photoelectron spectroscopy (XPS) spectra were recorded using the ESCALAB 220XL instrument. The X70 steel disks were submerged in a 100 mg/L XCAE solution in a 1M HCl. All the parameters of XPS analysis have been described by earlier research. ^{10–12}

4. Results and Discussion

The phytochemical study reveals that tannins, flavonoids, and phenols are present in the acetate extract of *Scorzonera undulata*. Table 2 displays the findings of the phytochemical examination of *Scorzonera undulata* acetate extract.¹³

 Table 2. Phytochemical analysis results of Scorzonera undulata

 plant extract.

TPC (μg GAE/mg)	435.72549±14.741134
TFC (μg QE/mg)	74.130719±3.5312268
Tanin	0.6288 ± 0.0098

TPC: Total Phenols, TFC: Total flavonoids. GAE: gallic acid, QE: quercetin

The Folin-Ciocalteu reagent was used to determine the total phenolic content (TPC) and flavonoid content (TFC) in the SUAc fraction, which were then expressed as gallic acid (GAE) and quercetin (QE) equivalents, respectively. The results of the assays show that the acetate extract of *Scorzonera undulata* (SUAc) is rich in polyphenols 435.72549±14.741134 mg eq.gallic ac/g (sample) and with regard to flavonoids and tannins values of 74.130719±3.5312268 mg eq. Quercetin /g and 0.6288±0.0098 were recorded.

4. 1. LC-MS/MS Analysis

Three compounds were detected in the LC-MS/MS analysis of the ethyl acetate extract of *scorzonera undulata* (Table 3).

Table 3. Three major molecules of acetate extract of scorzonera undulata using LC-MS/MS analysis.

Name	Formula	MW	RT	
3',4',5-trihydroxy-6,7- dimethoxy-flavone (Cirsiliol)	$C_{17}H_{14}O_7$	330.0737	5.65	
4,5-Dihydroxy-6,7- dimethoxyflavone (Skrofulein)	C ₁₇ H ₁₄ O ₆	314.0082	7.13	
2S,3S,4aS,5aS,9aS,10aS)-3,5a, $C_{18}H_{32}O_7$ 360.2145 10.21 10a-Tris(methoxymethyl)-2-methyldecahydro-2H-dipyrano[3,2-b:2',3'-e] pyran-3-ol				

MW: molecular weight; RT: retention time

4. 2. Electrochemical Measurement

4. 2. 1. Potentiodynamic Polarization

Fig. 1 displays the cathodic and anodic polarization curves of X70 steel in 1M HCl medium in both the absence and the presence of various concentrations of the extract of *Scorzonera undulata* at 298 K. For Table 4, it lists the

(2S, 3S, 4aS, 5aS, 9aS, 10aS)-3, 5a, 10a-Tris (methoxymethyl)-2methyldecahydro-2H- dipyrano [3, 2-b: 2, 3'-e] pyran-3-ol

4, 5-Dihydroxy-6, 7-dimethoxyflavone (Skrofulein)

3', 4', 5-trihydroxy-6, 7-dimethoxy-flavone (Cirsiliol)

Fig 1. Different compounds present in Scorzonera undulata.

electrochemical characteristics derived from the polarization curves, including recovery rate, corrosion inhibition efficiency EI (%), corrosion current density (I_{corr}), corrosion potential (E_{corr}), cathodic and anodic Tafel constants (β_c and β_a), and others.

Inhibitory efficacy is defined as follows:

$$EI\% = \frac{(i_0 - i_{inh})}{i_0} \times 100$$
 (1)

where i₀ and i_{inh} are the values of the steel's corrosion current density after immersion in an acidic medium, respectively without and with the addition of an inhibitor, as extrapolated from the cathodic or anodic lines of Tafel. A first analysis of these curves shows that there is a reduction of the corrosion potential as the inhibitor concentration

increases. The addition of the inhibitor in solution induces a significant decrease of both anodic and cathodic partial currents.

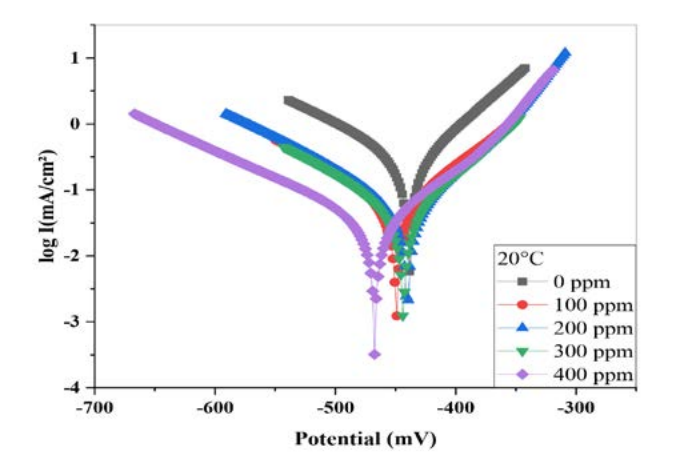


Fig 2. Polarization curves of X70 steel in solution at 1 M HCl and different SUAc concentrations.

Table 4. Electrochemical parameters of X70 steel in 1M HCl without and with the addition of different concentrations at 298K temperature of the *Scorzonera undulata* extract.

C (mg L	E -1) (mV)	i _{corr} (mA.cm ⁻²)	$\begin{array}{c} R_p \\ \Omega cm^2 \end{array}$	β _a (mV.dec ⁻¹	– β _c)(mV.dec [–]	EI 1) (%)
0	-438.9	0.2019	62.37	62.7	90.9	_
100	-449.4	0.0754	284.57	89.1	114.3	62.65
200	-440.3	0.0661	321.59	65.6	112.5	67.26
300	-443.6	0.053	370.42	73	107.1	73.75
400	-467.3	0.0332	579.57	77.7	124.3	83.56
500	-463.8	0.0462	205.58	53.7	97.6	77.12

The active area of the electrode decreases as the inhibitor concentration and the inhibitory efficiency rise, and the adsorbed film can exhibit ohmic behavior. When the inhibitor is present, the reaction of hydrochloric acid reduction and dihydrogen release might proceed according to the same mechanism.

In relation to the polarization of the steel in 1M HCl, the slope of the anodic Tafel line (β_a) is 62.7 mV. The βa value represents a reduction in oxidation current density when an inhibitor is present. 14 this outcome demonstrates unequivocally the anodic and cathodic effects of our inhibitor. The results show that the active sites on the metal surface are being blocked by the adsorbed molecules of the extract, decreasing the corrosion current density, $^{15-16}$ with a maximum efficiency of 83.56 % at 400 mg L $^{-1}$. The addition of this inhibitor results in a decrease in the cathodic and anodic current densities without modifying the corrosion potential value, according to the cathodic and anodic the polarization curves.

4. 3. Electrochemical Impedance Spectroscopy

Fig.3 shows Nyquist diagrams of steel immersed in acid solution with and without the addition of different inhibitor doses.

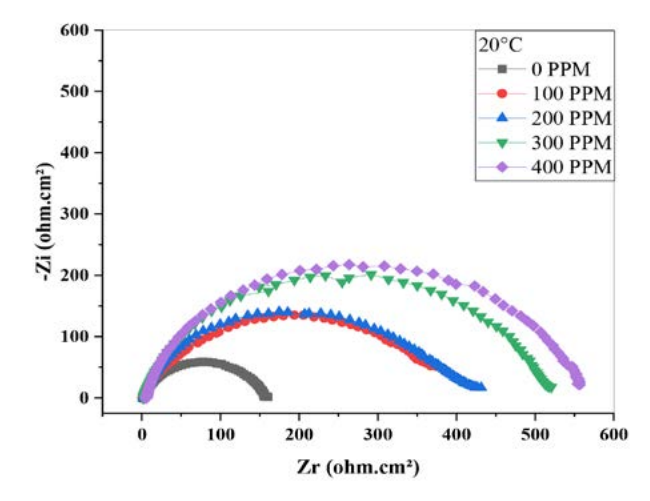


Fig 3. Electrochemical impedance of steel X70 in solution with 1 M HCl and different concentrations of SUAc (Representation in the *Nyquist* plane).

According to the following relationship, the load transfer resistance is used to calculate how well steel resists corrosion:

$$EI\% = \frac{(R_{tinh} - R_t)}{R_{tinh}} \times 100 \tag{2}$$

where R_t and Rtinh represent the steel's load transfer resistances after immersion, without and with the inhibitor added, respectively. Table 5 summarizes the electrochemical impedance spectroscopy (EIS) results for the inhibitory efficiency and electrochemical parameters for various concentrations of steel corrosion inhibitor in 1M HCl medium¹⁷.

Table 5. At various concentrations of SUAc extract, electrochemical impedance characteristics were measured in both the absence and the presence of the inhibitor.

C (mg L ⁻¹)	R_t (Ωcm^2)	$C_{ m dl}$ ($\mu F m cm^{-2}$)	EI %
0	156.5	56.91	-
100	395.6	254.2	60.44
200	413.6	86.19	62.16
300	514.7	77.29	69.59
400	557.9	31.94	71.95
500	257.4	69.22	39.20

The evaluation of these findings prompts us to make the following conclusions:

A single capacitive loop being present. This kind of graph often shows that a charge transfer process regulates the breakdown of carbon steel. 18–19 It is obvious that add-

ing SUAc extract causes the loops to grow in size, which increases their resistance to the medium's corrosiveness. This behavior might be brought on by the development of a shield once the inhibitors have been absorbed onto the steel surface.

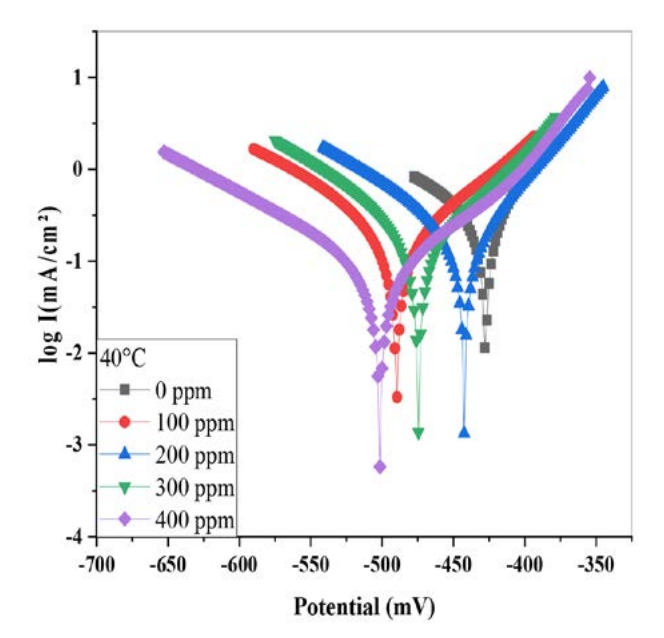
The area of active sites on the metal surface appears to decrease when inhibitor concentration is increased. This decrease may be due to the blocking of the active surface by adsorption of the inhibitor on the metal surface and consequently the increase of the transfer resistance $R_{\rm t}$ which gives a maximum inhibitory efficiency of 71. 95% at 400 mg $L^{-1}.$

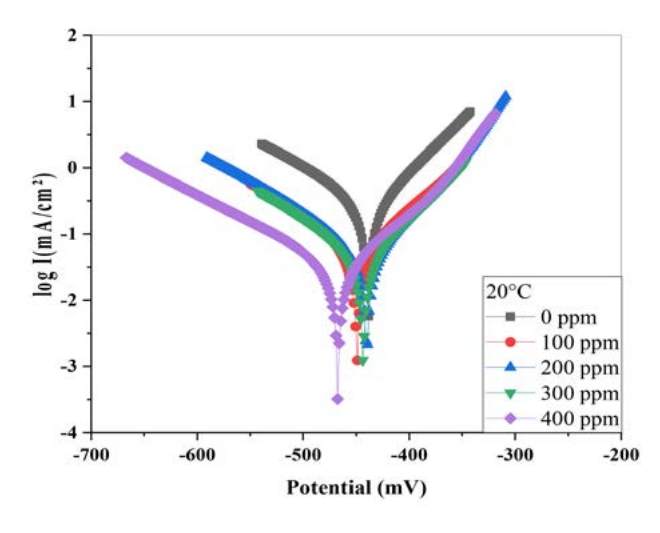
As the concentration of SUAc rises, the charge transfer resistance also increases (Table 5). This can be explained by a strengthening of the most inhibitive oxide layer's protective qualities, which causes a rise in R_t values. The impedance study and polarization measurement's results are therefore in good accord²⁰.

4. 4. Effect of Temperature

One of the factors that can alter a material's response to a corrosive environment is temperature. At different temperature, the identical electrochemical tests on X70 steel in 1 M HCl solution were carried out in both the absence and the presence of the inhibitor (298 K, 308 K and

318 K). Table 6 lists the values for the corrosion potential (E_{corr}), corrosion current density (i_{corr}), anode βa and cathode βc slopes, and inhibitor efficiency (EI). It appears that as the temperature increases, the corrosion current density increases while the inhibition efficiency decreases.





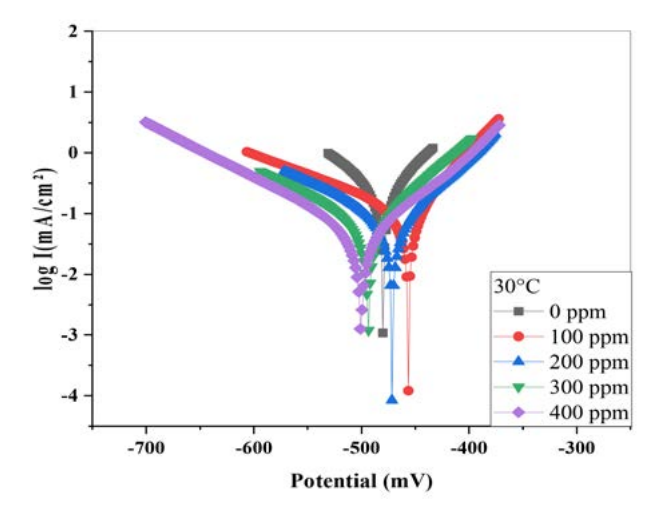
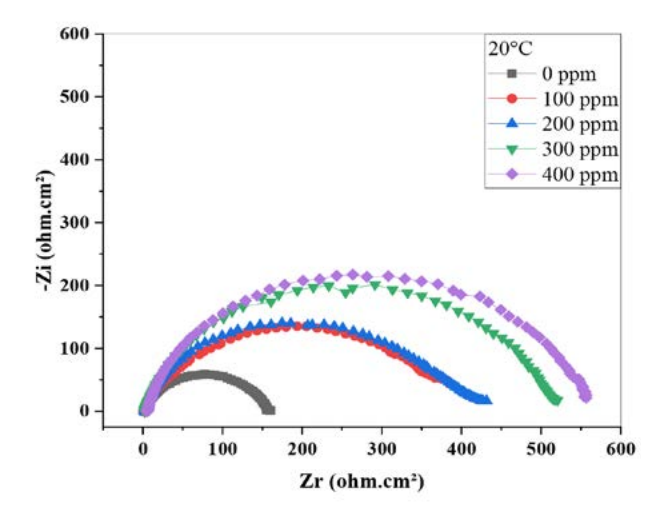
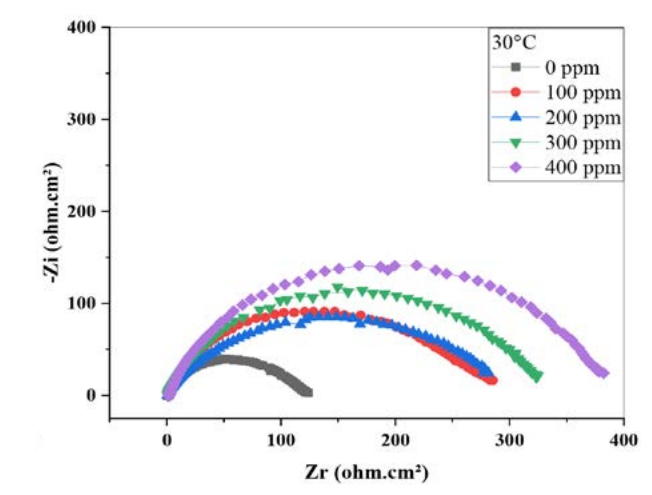


Fig 4. Curves of polarization in 1 M HCl at various temperatures in the presence and the absence of an inhibitor.

Table 6. Electrochemical parameters of 1 M HCl and inhibitor at dif	fferent temperatures
--	----------------------

Electrolyte	Temperatures	E _{corr} (mV)	i _{corr} (mA.cm ⁻²)	$R_p \over \Omega cm^2$	β_a (mV.dec ⁻¹)	$-\beta_c (mV.dec^{-1})$	θ (%)	EI
HCl 1M	298	-438.9	0.2019	62.37	62.7	90.9	_	_
	308	-480.1	0.2392	56.81	67.1	82.8	_	_
	318	-427.5	0.2764	46.32	56.1	103.4	_	_
Extract	298	-467.3	0.0332	579.57	77.7	124.3	0.8356	83.56
	308	-500.5	0.0492	377.74	71.6	110.7	0.7943	79.43
	318	-501.7	0.0799	239.96	71.8	116.6	0.7109	71.09





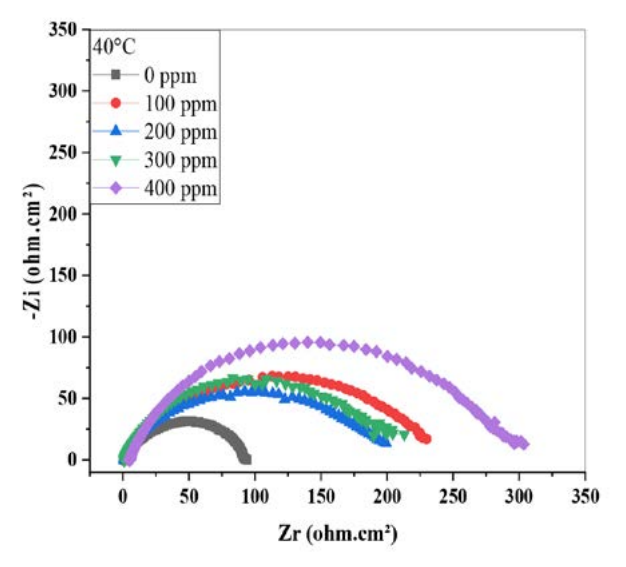


Fig 5. SIE curves obtained at different temperatures (20, 30 and 40 $^{\circ}C$)

Fig. 5 shows the impedance diagrams obtained at different temperatures (20, 30 and 40 °C), showing a pattern of the diagrams that is not modified by temperature; however, the size of

the capacitive loop decreases with increasing temperature. These results are in a good agreement with the results obtained from the polarization curves.

Table 7. Results of electrochemical impedance tests in 1M HCl at different temperatures without and with the addition of 400 mg L⁻¹ of SUAc.

Electrolyte	Temperatures (K)	R (Ωcm²)	C_{dl} ($\mu F cm^{-2}$)	EI %
	298	37.28	213.4	_
HCl 1M	308	119.7	106.2	_
	318	94.84	106	_
	298	557.9	31.94	76.14
Extract	308	384.8	92.63	72.10
	318	306.1	116.4	69.02

4. 5. Thermodynamic Study

The variation laws of the adsorbed quantity, as a function of inhibitor concentration, can often be represented by different types of 4, 4' isotherms.

Table 8. Correlation coefficient.

Isotherm		\mathbb{R}^2	
T	20 °C	30 °C	40 °C
Langmuir	0.996	0.999	0.990
Temkin	0.963	0.94	0.927
Fremkin	0.622	0.574	0.526
Freundlich	0.984	0.92	0.91

Langmuir:
$$\frac{c}{\theta} = \frac{1}{K} + C$$
 (3)

Temkin:
$$\theta = \frac{1}{\alpha} \times \text{Ln}(K \times C)$$
 (4)

Freundlich:
$$Ln\theta = Ln K + \propto Ln C$$
 (5)

According to the variation in the recovery, rate (C/θ) as a function of the concentration of SUAc at various temperatures, the plot of the Langmuir isotherm is shown in Fig. 6.

The values of the adsorption constants (K_{ads}) , adsorption energies (ΔG°_{ads}) , enthalpy (ΔH°_{ads}) and entropies (ΔS°_{ads}) are grouped in Table 9.

Table 9. Thermodynamic parameters related to the adsorption of SUAc on the surface of X70 steel.

Temperatures		ΔG° _{ads} (kJ mol ⁻¹)	ΔH° _{ads} (kJ mol ⁻¹)	$\begin{array}{c} \Delta S^{\circ}_{ads} \\ (J \ mol^{-1} K^{-1}) \end{array}$
20°C	0.016975	-18.42		-18.4006
30°C	0.014428	-18.32	-23.9	-18.4282
40°C	0.010681	-18.14		-18.4065

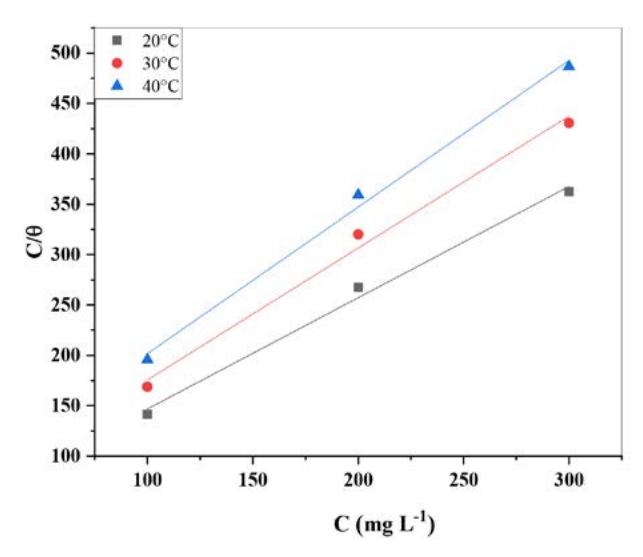


Fig 6. Langmuir adsorption isotherm of SUAc on the surface of steel X70 in the 1M HCl solutions at different temperatures.

The spontaneity of the adsorption process and the durability of the double layer adsorbed on the metal surface are shown by the negative values of the free energy of adsorption $(\Delta G^{\circ}_{ads}).^{21}$ Typically, the electrostatic interactions between the charged molecules and the charged metal are what cause the values of ΔG°_{ads} to be close to or less than –20 kJ/mol (physical adsorption). SUAc is physisorbed on the metal surface, as shown by the predicted values of ΔG°_{ads} near to –20kJ mol $^{-1}$ (Table 9).

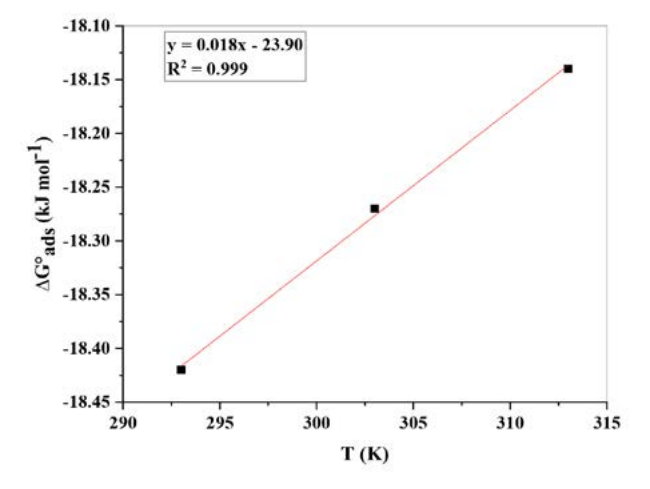


Fig 7. Variation of the adsorption free energy ($\Delta G^{^{o}}_{ads})$ as a function of the temperature.

The apparent activation energy (thermodynamic parameters relating to the dissolution of steel X70 in solution)

The activation energy for the various concentrations of SUAc is higher according to the data shown in Table 10

than the activation energy without the addition of SUAc. This higher activation energy is due to the extract's physisorption on the surface of X70 steel.^{22–25}

Table 10. Parameters of carbon steel's activation energy in an acidic solution, both with and without SUAc present in varied concentrations

C (mg L ⁻¹)	E _a (kJ mol ⁻¹)
0	13.05
100	24.11
200	24.67
300	26.95
400	36.49

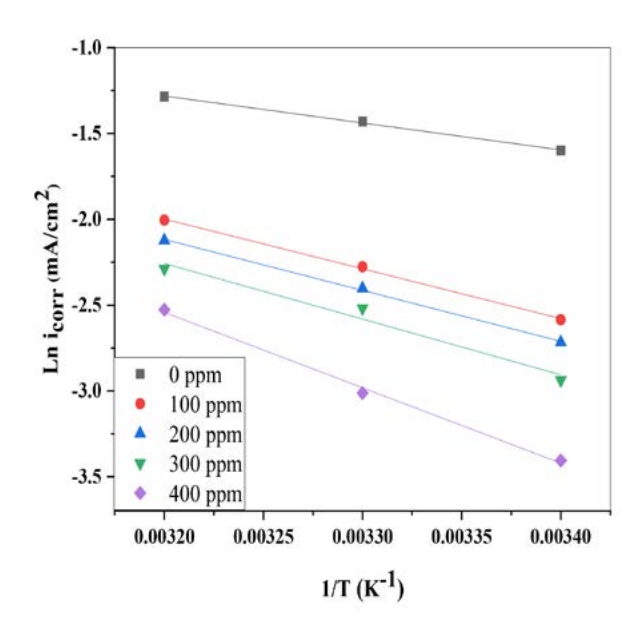


Fig 8. Graph of $\ln{(i_{corr})}$ in the presence and absence of SUAc as a function of the temperature's inverse.

4. 6. Morphological Investigation

In both the absence and the presence of a plant extract, top view SEM micrographs of carbon steel submerged in 1 M HCl are shown in Fig. 9. Without plant extract, the carbon steel specimen's SEM picture reveals an uneven, acid-damaged surface. It is very clear from Fig. 8 that the addition of the inhibitor under study (SUAc) to the corrosive medium stops the dissolution and consequently the corrosion of the metal. The creation of a protective layer by the SUAc extract on the surface of the steel is thought to be the cause of this visual variation. ^{26–27}

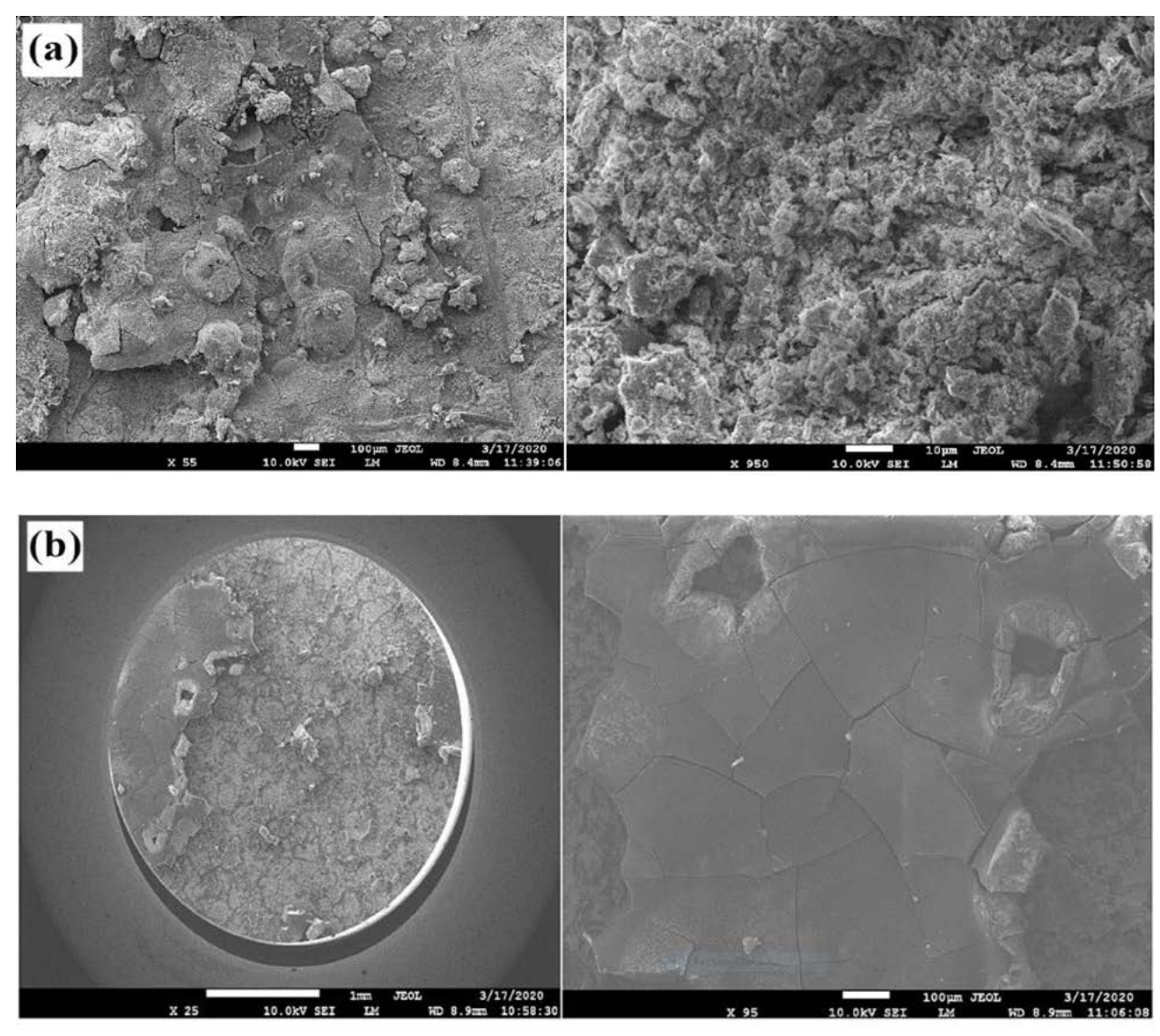


Fig 9. SEM top view images of carbon steel in acidic solution: (a) in absence of SUAc and (b) in presence of SUAc.

4. 7. XPS (X-ray Photoelectron Spectrometry)

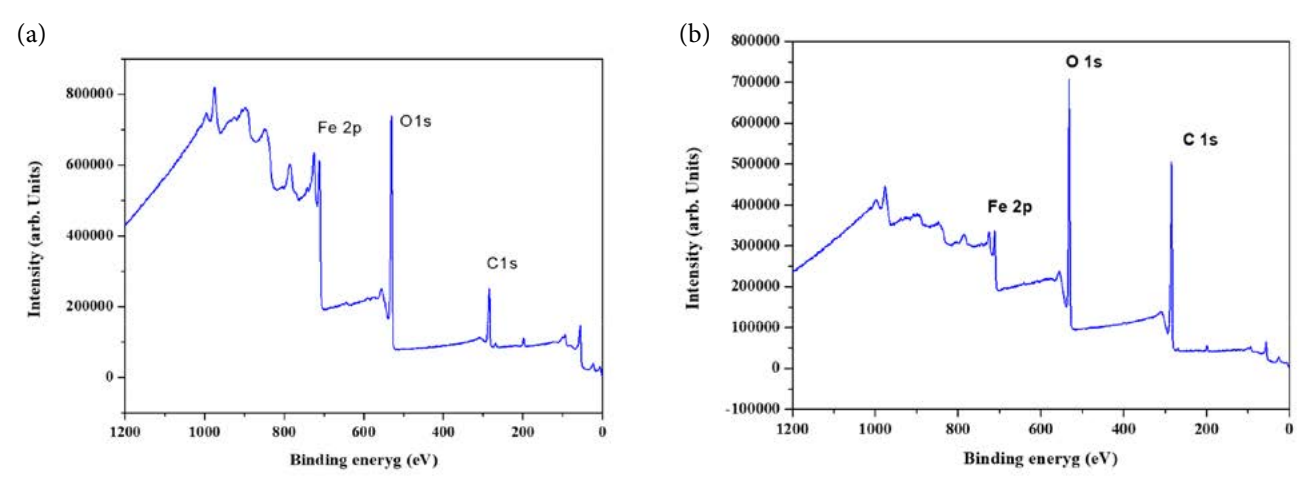
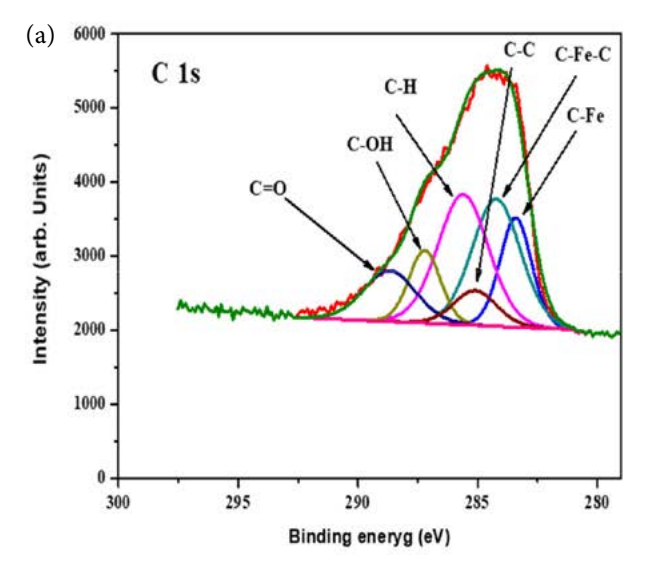


Fig 10. XPS survey spectra (a) without and (b) with SUAc.

Fig. 10 displays the XPS survey spectra of the films before and after SUAc treatment. All samples' surfaces include carbon (C), iron (Fe), and oxygen as would be expected (O). Though no nitrogen impurities were found in either sample, it is significant to note that the CNW films that have not been treated have a higher concentration of O impurities. Therefore, it is believed that the increase of the O amount before the use of SUAc is due to the higher surface oxidation.

bonds (Fe-C....), which indicates a surface passivation by an amorphous carbon layer especially with the increase of C-H amount. The appearance of new bond O-C-OH after the use of SUAc indicates the presence of hydroxyl groups probably originates from the SUAc inhibitor.

The O1s core level envelope in the XPS spectra of the sample without SUAc (Fig.12 (a)) may be deconvoluted into three component peaks known as O1, O2, and O3. The Fe-O bonds in the FeOx lattice are typically credited with



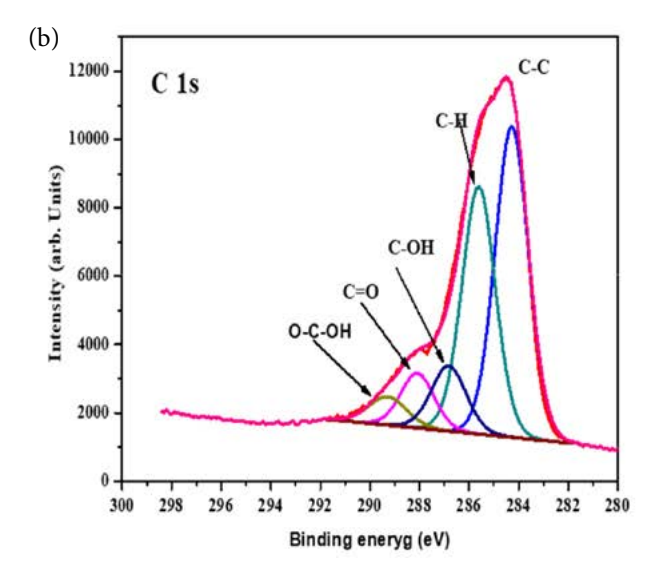
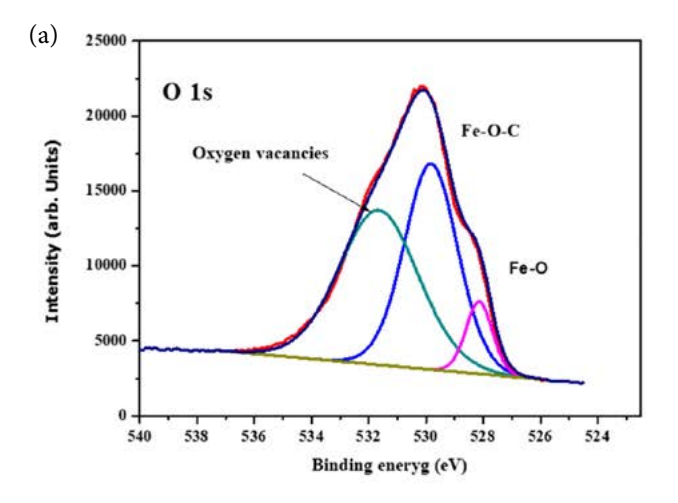


Fig 11. XPS C1s higher resolution spectra of sample (a) without and (b) with SUAc.

The sample's C 1s higher resolution de-convoluted XPS spectra with and without SUAc are shown in Fig. 11. The (Fe-C), C-Fe-FeC C, C-C, C-H, C OH, and (C O) C OH) bonds on the surface of the carbide phase are responsible for the peaks at 283.2, 284.4, 286.1, 288.1, and eV, respectively, in Fig. 10(a). The task outlined in the literature, ^{28–30} can be compared to these binding energies. After the use of SUAc, it can be observed the disappearance of the carbide

producing the O1 component, which is located at about 528.0 eV on the low binding energy (BE) side of the O 1s spectrum. The O2 component can be assigned to the Fe-O-C bond, whereas the O3 component can be attributed to oxygen vacancies. Its intensity is a measurement of the number of oxygen atoms around the oxidized iron. With the addition of SUAc, the Fe-O-C peak disappear (Fig.12 (b)) in accordance with the XPS analysis of C1s spectra.



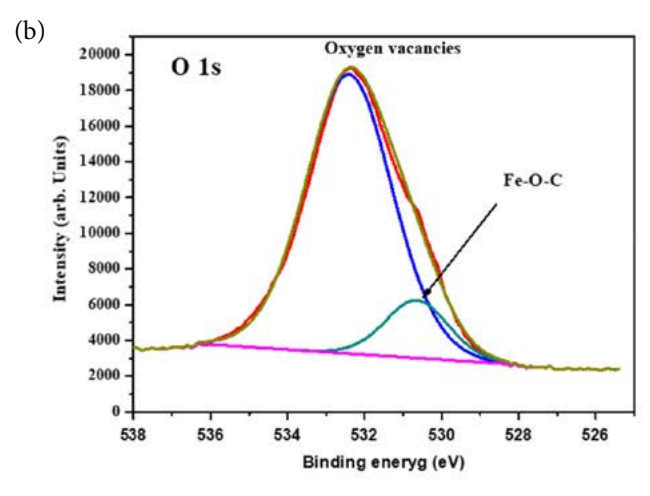
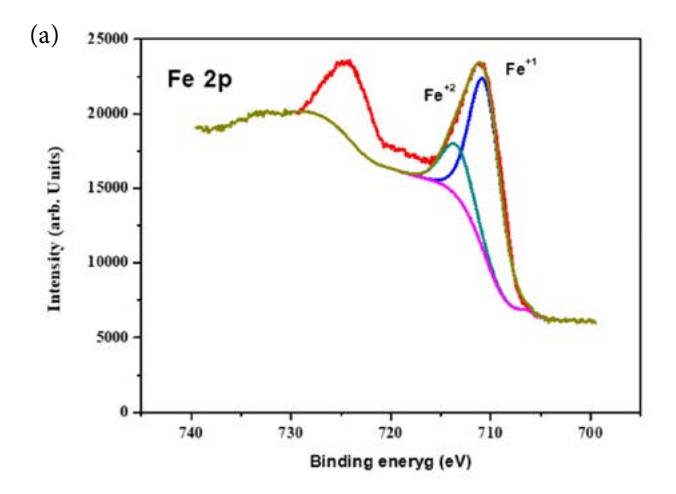


Fig 12. XPS O1s higher resolution spectra of sample (a) without and (b) with SUAc.



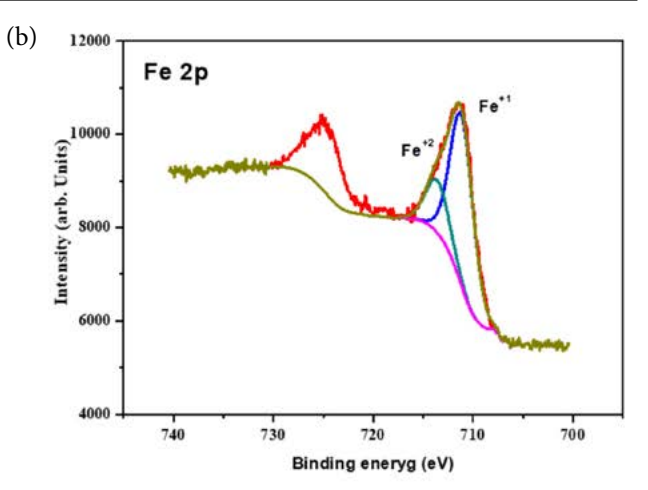


Fig 13. XPS Fe2P higher resolution spectra of sample (a) without and (b) with SUAc.

The XPS study spectra before and after the SUAc treatment are shown in Fig. 13, the surfaces of all samples contain iron (Fe^{2+}) , and $(Fe^{+1})^{31}$.

5. Conclusion

This study presents the inhibitory impact and adsorption behavior of a *Scorzonera undulata* ethyl acetate extract on X70 steel in a 1M HCl media. Tafel plots have shown that the extract is an excellent mixed inhibitor. Additionally, the data show that the effectiveness of the inhibition rises with extract concentration, reaching a maximum of 83% at 400 ppm *Scorzonera undulata*. The extract remained active at the studied temperatures range. Finally, the obtained thermodynamic parameters revealed a physical adsorption between the extract and the metal surface. The inhibitor molecules interact with the mild steel surface strongly, as evidenced by the Gibbs free energy of adsorption's (ΔG_{ads}°) negative value.

Conflict of Interest

The authors declare that they are responsible for the content and writing of the article.

The authors also declare that they have no conflict of interest with suggested reviewers.

6. References

- M. Goyal, S. Kumar, I. Bahadur, C. Verma, E. E. Ebenso. *J. Mol. Liq.* 2018, 256, 565–573. DOI:10.1016/j.molliq.2018.02.045
- T. Gu, Z. Chen, X. Jiang, L. Zhou, Y. Liao, M. Duan, H. Wang, Q. Pu. *Corros. Sci.* 2015, 90, 118–132.
 DOI:10.1016/j.corsci.201 4.10.004 640.
- 3. R. Yıldız. *Corros. Sci.* **2015**, *90*, 544–553. **DOI:**10.1016/j.corsci.2014.10.047

- A. Zarrouk, B. Hammouti, T. Lakhlifi, M. Traisnel, H. Vezin, F. Bentiss. *Corros. Sci.* 2015, 90, 572–584.
 DOI:10.1016/j.corsci.2014.10.052
- N. I. Kairi & J. Kassim.. Int J Electrochem Sci. 2013, 8, 7138–7155.
- 6. V. G. Vasudha, & P. K. Shanmuga. Res. J. Chem. Sci. 2013, 3, 21–26
- 7. J. Halambek, I. Cindrić, & A. N. Grassino. Carbohydr. Polym. 2020, 234. **DOI:**10.1016/j.carbpol.2020.115940
- 8. K.R. Markham. Techniques of flavonoids identification. Ed Academic Press., 1982, 6100.
- 9. J. Bruneton, Pharmacognosie, phytochimie des plantes medicinales . 2 édition, Tec et Doc (Ed.), Paris, 1993,914.
- M. Outirite, M. Lagrenée, M. Lebrini, M. Traisnel, C. Jama,
 H. Vezin, F. Bentiss. ac. *Electrochim. Acta.* 2010, 55, 1670–1681. DOI:10.1016/j.electacta.2009.10.048
- M. Lebrini, M. Lagrenée, H. Vezin, M. Traisnel, F. Bentiss. Corros. Sci. 2007, 49, 2254–2269.
 DOI:10.1016/j.corsci.2006.10.029
- 12. E. Ituen, O. Akaranta, A. James, S. Sun. Sustainable Mater. *Technol.* **2017**, *11*, 12–18. **DOI:**10.1016/j.susmat.2016.12.001
- V. L. Singleton, J. A. Rossi. Am. J. Enol. Vitic. 1965, 16, 144– 158.
- A. Dehghani, G. Bahlakeh, B. Ramezanzadeh, M. Ramezanzadeh. *J. Mol. Liq.* 2019, 277, 895–911.
 DOI:10.1016/j.molliq.2019.01.008
- B. R. Linter & G. T. Corros. Sci. 1999, 41, 117–139.
 DOI:10.1016/S0010-938X(98)00104-8
- Da Silva, M.V.L.; de BrittoPolicarpi, E.; Spinelli, A. *J. Taiwan Inst. Chem. Eng.* 2021, *129*, 342–349
 DOI:10.1016/j.jtice.2021.09.026
- 17. Kaur, J.; Daksh, N.; Saxena, A. *Arab. J. Sci. Eng.* **2022**, *47*, 57–74. **DOI**:10.1007/s13369-021-05699-0
- M. Lebrini, F. Robert, A. Lecante, C. Roos, Corros. Sci. 2011, 53, 687–695. DOI:10.1016/j.corsci.2010.10.006
- Abbout, S.; Chebabe, D.; Zouahri, M.; Rehioui, M.; Lakbaibi,
 Z.; Hajjaji, N. *J. Mol. Struct.* 2021,1240, 130611
 DOI:10.1016/j.molstruc.2021.130611

- Khadom, A. A.; Kadhim, M. M.; Anaee, A. R.; Mahood, H. B.; Mahdi, M. S.; Salman, A. W.J. Mol. Liq. 2021, 343,116978
 DOI:10.1016/j.molliq.2021.116978
- M. M. Solomon, S. A. Umoren, I. I. Udosoro, A. P. Udoh. Corros. Sci. 2010, 52, 1317–1325. DOI:10.1016/j.cors-ci.2009.11.041. DOI:10.1016/j.corsci.2009.11.041
- K.Tebbji, N.Faska, A.Tounsi, H.Oudda, M. Benkaddour, B.Hammouti, *Mater. Chem. Phys.* 2007, 106, 260–267.
 DOI:10.1016/j.matchemphys.2007.05.046
- X. Li, S. Deng, H. Fu. Corros. Sci. 2012, 62, 163–175.
 DOI:10.1016/j.corsci.2012.05.008
- K. Ramya, R. Mohan, K. K. Anupama, & A. Joseph. *Mater. Chem. Phys.* 2015, *149*, 632–647.
 DOI:10.1016/j.matchemphys.2014.11.020
- 25. Hamdy, A.; El-Gendy, N. S. *Egypt. J. Pet.* **2013**, *22*, 17–25. **DOI:**10.1016/j.ejpe.2012.06.002

- 26. R. Laamari, J. Benzakour, F. Berrekis, A. Villemin. Les Technologies de Laboratoir. **2010**, *5*, 18–25.
- J. Zhang, X. L. Gong, H. H. Yu, M. Du. Corros. Sci. 2011, 53, 3324–3330. DOI:10.1016/j.corsci.2011.06.008
- 28. Alibakhshi, E.; Ramezanzadeh, M.; Bahlakeh, G.; Ramezanzadeh, B.; Mahdavian. M.; Motamedi, M.J. Mol. Liq. 2018, 255, 185–198. DOI:10.1016/j.molliq.2018.01.144
- C. T. Wirth, S. Hofmann, J. Robertson. *Diam. Relat. Mater.* 2009, 18, 940–945. DOI:10.1016/j.diamond.2009.01.030
- G. J. Kovacs, I. Bertóti, G. Radnóczi. *Thin Solid Films.* 2008, 516, 7942–7946. DOI:10.1016/j.tsf.2008.06.005
- D. Yang, A. Velamakanni, G. Bozoklu, S. Park, M. Stoller, R. D. Piner, R. S. Ruoff. *Carbon*. **2009**, *47*, 145–152.
 DOI:10.1016/j.carbon.2008.09.045

Povzetek

Za ogljikovo jeklo X70 v 1 M raztopini klorovodikove kisline je bil raziskan acetatni ekstrakt *Scorzonera undulata* (SU-Ac) kot ekološki inhibitor korozije. Protikorozijski učinek izvlečka *Scorzonera undulata* je bil preučevan s potenciodinamično polarizacijsko analizo in elektrokemijsko impedančno spektroskopijo (EIS). Polarizacijske krivulje jasno kažejo, da je ekstrakt odličen mešani inhibitor. Ugotovitve dodatno kažejo, da je največja učinkovitost inhibicije v vrednosti 83 % dosežena s koncentracijo inhibitorja do 400 mg/L pri 298 K. Langmuirjevi izotermi sledi adsorpcija inhibitorja na jekleni površini po mehanizmu fizične adsorpcije. Za razumevanje inhibitornega mehanizma so bili določeni termodinamični (ΔG°_{ads}) in aktivacijski parametri (E_a , ΔH_a in ΔS_a). Dodatno so bile opravljene študije površinske kemije in morfologije z vrstično elektronsko mikroskopijo (SEM) in rentgensko fotoelektronsko spektrometrijo. Rezultati kemijskih in elektrokemijskih meritev potrjujejo, da se na površini ogljikovega jekla tvori zaščitni film.



Except when otherwise noted, articles in this journal are published under the terms and conditions of the Creative Commons Attribution 4.0 International License